THE JOURNAL OF BIOLOGICAL CHEMISTRY
Vol. 279, No. 43, Issue of October 22, pp. 44621–44627, 2004

Printed in U.S.A.

The Chloroplast Rieske Iron-Sulfur Protein

AT THE CROSSROAD OF ELECTRON TRANSPORT AND SIGNAL TRANSDUCTION*

Received for publication, June 22, 2004, and in revised form, August 5, 2004
Published, JBC Papers in Press, August 16, 2004, DOI 10.1074/jbc.M406955200

Catherine de Vitry‡§, Yexin Ouyang¶, Giovanni Finazzi‡, Francis-André Wollman‡, and Toivo Kallas¶

From the ‡Physiologie Membranaire et Moléculaire du Chloroplaste CNRS UPR 1261, Institut de Biologie Physico-Chimique, 13 Rue Pierre et Marie Curie, 75005 Paris, France and ¶Department of Biology and Microbiology, University of Wisconsin, Oshkosh, Wisconsin 54901

We have addressed the functional and structural roles of three domains of the chloroplast Rieske iron-sulfur protein; that is, the flexible hinge that connects the transmembrane helix to the soluble cluster-bearing domain, the N-terminal stromal protruding domain, and the transmembrane helix. To this aim mutants were generated in the green alga *Chlamydomonas reinhardtii*. Their capacities to assemble the cytochrome b_6f complex, perform plastoquinol oxidation, and signal redox-induced activation of the light-harvesting complex II kinase during state transition were tested *in vivo*. Deletion of one residue and extensions of up to five residues in the flexible hinge had no significant effect on complex accumulation or electron transfer efficiency. Deletion of three residues (Δ3G) dramatically decreased reaction rates by a factor of ~10. These data indicate that the chloroplast iron-sulfur protein-linking domain is much more flexible than that of its counterpart in mitochondria. Despite greatly slowed catalysis in the Δ3G mutant, there was no apparent delay in light-harvesting complex II kinase activation or state transitions. This indicates that conformational changes occurring in the Rieske protein did not represent a limiting step for kinase activation within the time scale tested. No phenotype could be associated with mutations in the N-terminal stromal-exposed domain. In contrast, the N17V mutation in the Rieske protein transmembrane helix resulted in a large decrease in the cytochrome *f* synthesis rate. This reveals that the Rieske protein transmembrane helix plays an active role in assembly-mediated control of cytochrome *f* synthesis. We propose a structural model to interpret this phenomenon based on the *C. reinhardtii* cytochrome b_6f structure.

The cytochrome (cyt)[1] b_6f complex couples electron and proton transfer in photosynthetic organisms. It catalyzes the oxidation of plastoquinol (PQH_2) and the reduction of plastocyanin. The complex contains four major subunits: cyt *f*, cyt b_6, Rieske protein, and subunit IV (for review, see Ref. 1). Four of its redox cofactors have long been identified; they are a *c*-type heme in cyt *f*, two *b*-type hemes in cyt b_6 (b_L and b_H), and an Fe_2S_2 cluster in the Rieske iron-sulfur protein (ISP). A new heme c_i (or *x*) bound to cyt b_6 close to the quinone reduction Q_i site, a chlorophyll, a carotenoid, and specific lipids have also been identified in the cyt b_6f structures from the green alga *Chlamydomonas reinhardtii* (*Chlamydomonas*) (2) and the cyanobacterium, *Mastigocladus laminosus* (3). Additional biochemical and spectroscopic characterization of heme c_i has been obtained recently (4).

The ISP is essential for PQH_2 docking and for diverting its electrons into the "high" and "low potential pathways." After PQH_2 oxidation at the Q_o site located close to the lumenal face of the thylakoid membrane, one electron is injected in the "high potential chain" consisting of the ISP, cyt *f*, and plastocyanin. This chain channels electrons from photosystem (PS) II to PS I. The second electron from PQH_2 is injected into the "low potential chain" comprised of the b_L, b_H, and likely the c_i hemes. This second pathway results in electron transfer across the membrane to the Q_i site, located close to the stromal face of the thylakoid membrane. According to the Q cycle mechanism (5, 6), the genesis of a PQH_2 at the Q_i site increases the H^+/e^- stoichiometry of electron flow. Diversion of electrons to the high and low potential branches is mediated by an ISP conformational change. In the related mitochondrial bc_1 cyt complexes, the rotational swing of the ISP extramembrane domain leads to a cluster movement over 20 Å, which prevents a double electron injection into the high potential chain (for review, see Ref.1). Evidence for this movement was provided by three-dimensional cyt bc_1 structures (7–9), electron paramagnetic resonance spectroscopy (10), and mutagenesis studies (for review, see Ref. 11). Several lines of evidence support an ISP domain movement in the b_6f complex; they are two-dimensional crystals (12), viscosity studies (13), electron transfer from ISP to cyt *f in vitro* (14), inhibitor binding (15), mutagenesis studies (Ref. 16 and the current work), and three-dimensional cyt b_6f structures (2, 3).

Besides modulating electron flow in photosynthesis, the ISP movement has been implicated in redox signaling during state transitions. State transitions are a mechanism for balancing the light absorption capacity of the two photosystems. Moreover, in *Chlamydomonas*, state transitions are also associated with a switch from linear to cyclic electron flow (for review, see Ref. 17). In chloroplasts, state transitions rely on the reversible phosphorylation of the PSII outer antenna complexes (LHCII) by a kinase that becomes activated when the plastoquinone pool becomes reduced (for review, see Ref. 18). Binding of PQH_2 to the Q_o site of the b_6f complex is required for LHCII kinase activation (19–21). ISP conformational changes have been pos-

* This work was supported by the CNRS, National Science Foundation Grant MCB 0091415, and University of Wisconsin-Oshkosh Faculty Development R788 grants (to T. K.). The costs of publication of this article were defrayed in part by the payment of page charges. This article must therefore be hereby marked "*advertisement*" in accordance with 18 U.S.C. Section 1734 solely to indicate this fact.

§ To whom correspondence should be addressed. Tel.: 33-1-58-41-50-55; Fax: 33-1-58-41-50-22; E-mail: catherine.devitry@ibpc.fr.

[1] The abbreviations used are: cyt, cytochrome; HG, Hecameg (6-*O*-(*N*-heptylcarbamoyl)-methyl-α-D-glycopyranoside); ISP, iron-sulfur protein; LHC, light-harvesting complex; PQH_2, plastoquinol; PSI, photosystem I; PSII, photosystem II; SQDG, sulfoquinovosyldiacylglycerol; WT, wild type; FCCP, carbonylcyanide-*p*-(trifluoromethoxy)phenylhydrazine; Tricine, *N*-[2-hydroxy-1,1-bis(hydroxymethyl)ethyl]glycine.

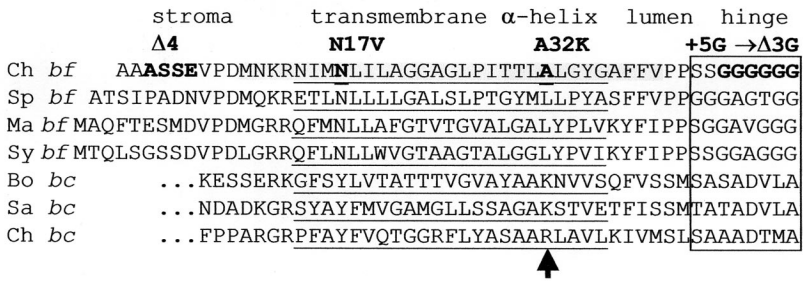

FIG. 1. **Mutations in the N-terminal, transmembrane, and flexible hinge domains of the *Chlamydomonas* Rieske ISP and alignment with partial sequences of other ISPs.** Shown is deletion of 4 residues in the stromal N terminus (*Δ4*) and diminution of α-helix polarity (*N17V*). Charge introduction at lumenal end of the α-helix (A32K) is indicated by an *arrow*. Flexible hinge glycine additions (+5G, +3G, +1G) and deletions (Δ1G, Δ3G) are shown. Transmembrane α-helices are *underlined*. The N-terminal α-helix detected in the *Chlamydomonas* b_6f structure is indicated in *gray* (2). Flexible hinges are *boxed*. *Ch*, *C. reinhardtii* (36); *Sp*, spinach; *Ma*, *M. laminosus* (3); *Sy*, *Synechococcus* sp. PCC 7002; *Bo*, bovine; *Sa*, *Saccharomyces cerevisiae*.

tulated to play a role in the activation process (21–23). However, the mechanisms that allow transduction of the activating signal from the lumenal to the stromal side of the membrane, where LHCII phosphorylation takes place, are not yet understood. *Chlamydomonas* LHC kinase has been cloned (24, 25), and a putative transmembrane helix is proposed. This helix might be directly involved in sensing PQH_2 binding to the Q_o site (22). Nonetheless, the existence of an intrinsic signaling pathway within the b_6f complex cannot be excluded.

Here, we performed an extensive mutagenesis study of the chloroplast ISP in *Chlamydomonas*. Our aim was to compromise its properties by various insertion/deletion/substitution in the flexible hinge, the N-terminal stromal-exposed, and the transmembrane domains and to test the consequences on electron transfer, kinase activation, and cyt b_6f complex assembly *in vivo*.

MATERIALS AND METHODS

Growth Conditions—Chlamydomonas strains were grown on Tris acetate-phosphate medium at pH 7.2 and 25 °C under 6 microeinsteins m^{-2} s^{-1} continuous illumination or in the dark and collected during the exponential phase at 2×10^6 cells ml^{-1}.

Site-directed Mutagenesis and Nuclear Transformation—Plasmid pACR4.5 (ampicillin-sensitive/tetracycline-resistant) containing the *Chlamydomonas PetC* gene (26) was used as the template for mutagenesis with the oligonucleotides: petC-Δ4,

5′-CGTTATGCCGGTGGTGCGCGCgGCCGCTGTGCCCGACATGAACAAGCGCAAC-3′; petC-N17V, 5′-CAAGCGCAACATCATGgtCCTGATCCTGGCTGGCTGGTGGCGCcGGTCTGCCATCAC-3′; petC-A32K, 5′-GCCCATCACCACCCTGaagCTGGGCTACGGcGCCTTCTTCGTGC; petC-+5G, 5′-CTACATTGTTCCTCTTTACAGCTCgGGCggcggtggcggtggcGGTGGCGGCGGTGGCCAG-3′; petC-+3G, 5′-CTACATTGTTCCTCTTTACAGCTCgGGCggcggtggcGGTGGCGGCGGTGGCCAG-3′; petC-+1G, 5′-CATTGTTCCTCTTTACAGCTCgggtGGCGGTGGCGGCGGTGGC-3′; petC-Δ1G, 5′-CATTGTTCCTCTTTACAGCTCgGGTGGCGGCGGCCAGGCC-3′; petC-Δ3G, 5′-CATTGTTCCTCTTTACAGCTCgGGCGGTGGCCAGGCCGCTAAG-3′.

Mutant plasmids, detected by restoration of ampicillin resistance, were subsequently screened for the NotI (petC-Δ4), NarI (petC-N17V, petC-A32K), or AvaI (petC-+5G, petC-+3G, petC-+1G, petC-Δ1G, petC-Δ3G) restriction sites, underlined in the above oligonucleotide sequences. *Chlamydomonas* double mutant cells with a cell wall deficiency (cw15) and a deletion in *PETC* (petC-Δ1 in de Vitry *et al.* (26); here referred to as ΔPetC) were transformed as in Kropat *et al.* (27) using HindIII-linearized plasmids. Phototrophic colonies were selected on minimal medium under light intensities of 40–100 microeinsteins m^{-2} s^{-1} and became visible after ~2 weeks. Transformants were characterized as in de Vitry *et al.* (26) by restriction analysis of specific PCR-amplified products (not shown). Mutations within the *Chlamydomonas PetC* gene were confirmed by DNA sequencing.

Protein Isolation, Separation, Analysis, and in Vivo Labeling—Thylakoid membranes were purified and resuspended in 10 mM Tricine-NaOH, pH 8.0, containing protease inhibitors (200 μM phenylmethylsulfonyl fluoride, 1 mM benzamidine, 5 mM ϵ-aminocaproic acid) as in Breyton *et al.* (28). Cyt b_6f complexes were extracted by a Hecameg (HG) solubilization (at 30 rather than 25 mM) of thylakoid membranes (29). Polypeptides were separated on 12–18% SDS-polyacrylamide gels containing 8 M urea (30). Lanes were loaded with equal amounts (15 μg) of chlorophyll. Proteins were electrotransferred onto Immobilon NC membranes in a semidry blotting apparatus at 0.8 $mA \cdot cm^{-2}$ for about 30 min. Immunodetection employed antisera raised against subunits of the *Chlamydomonas* cyt b_6f complex (cyt *f*, Rieske protein, cyt b_6) at a 1/200 dilution, and bands were visualized with ^{125}I-labeled protein A (28). Whole cells grown to 2×10^6 cells/ml were pulse-radiolabeled in the presence of 5 μCi/ml [^{14}C]acetate for either 5 min in the presence of 8 μg/ml cycloheximide (an inhibitor of cytoplasmic translation) or 8 min in the presence of 200 μg/ml chloramphenicol (an inhibitor of chloroplast translation) (30). Labeling was terminated by dilution of the isotope with 10 volumes of chilled 50 mM sodium acetate before thylakoid membrane isolation.

In vivo phosphorylation was performed as described in Wollman and Delepelaire (31) using [^{33}P]orthophosphate instead of [^{32}P]orthophosphate (21). Cells were grown to 2×10^6 cells/ml were harvested and resuspended in a phosphate-depleted medium for 30 min, then 2 μCi/ml [^{33}P]orthophosphate was added for 90 min. Cells were harvested, resuspended in a phosphate-depleted medium, and adapted for 30 min to state I conditions (plastoquinone pool-oxidized; cells were strongly agitated in the dark). To obtain state II conditions (plastoquinone pool-reduced), cells were incubated with 5 μM carbonylcyanide-*p*-(trifluoromethoxy)phenylhydrazone (FCCP) in the dark without agitation for 30 min (32). Phosphorylation and dephosphorylation reactions were stopped by the addition of 10 mM NaF and rapidly cooled to 4 °C before thylakoid membrane isolation.

Absorption and Fluorescence Spectroscopy—For spectroscopic analysis, cells were collected and re-suspended in 20 mM Hepes-NaOH, pH 7.2, in the presence of 20% Ficoll to prevent cell sedimentation. Measurements were performed at room temperature with a home-built spectrophotometer (33) as described in de Vitry *et al.* (26). cyt *f* and b_6 reduction was measured as the absorption changes at 554 and 564 nm, respectively, minus a base line drawn between 545 and 573 nm (34). The slow phase (phase b) of the electrochromic shift of carotenoids, which reflects charge transfer across the membrane and cyt b_6f catalysis, was measured at 515 nm. Non-saturating actinic flashes were employed to prevent multiple turnovers of the cyt b_6f complex. When required, FCCP was added at the concentration of 1 μM to collapse the electrochemical proton gradient.

State I-II transitions were measured according to the procedure previously employed (35); cells were adapted in the dark for 40 min in the presence of glucose oxidase (2 mg/ml), glucose (20 mM), and 3-(3′,4′-dichloroprenyl)-1–1-dimethylurea (10 μM), to obtain state II. Cells were then illuminated with continuous light (590 ± 10 nm, 60 microeinsteins m^{-2} s^{-1}) for 10 min to promote reversal to state I and to probe the state II to I transition. The same cells were then placed into darkness with periodic sampling to probe relaxation back to state II. This procedure allowed a true estimation of the state I-state II transition independent of other metabolic changes that accompany the aerobiosis- anaerobiosis transition.

RESULTS

Location of Mutations in the Rieske Protein N-terminal, Transmembrane, and Hinge Domains—Fig. 1 shows the locations of mutations that were introduced into the Rieske ISP of *Chlamydomonas* (36) and their alignment with partial sequences of other cyt b_6f and bc_1 Rieske proteins. Their locations

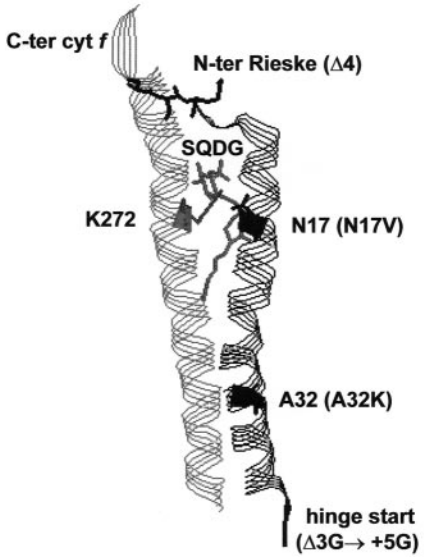

FIG. 2. **Mutations in the N-terminal, transmembrane, and flexible hinge of the Rieske protein in the *Chlamydomonas* b_6f complex structure.** The N-terminal domain of the Rieske protein (*N-ter Rieske*) is close to the C-terminal domain of cyt *f* (*C-ter cyt f*). An endogenous sulfolipid (SQDG) interacts with the Rieske protein Asn^{17} and cyt *f* Lys^{272} residues.

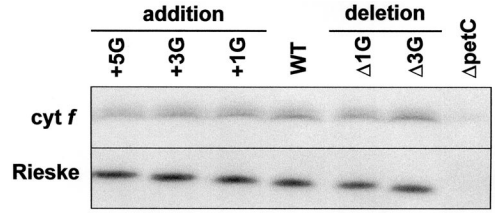

FIG. 3. **Accumulation of cyt b_6f subunits in the Rieske ISP flexible hinge mutants.** Cells from the exponential phase of growth were analyzed by SDS-PAGE (12–18% acrylamide, 8 M urea). Cyt *f* and Rieske protein were immunodetected. WT and Rieske deletion mutant (ΔpetC) strains are shown as controls.

within the N-terminal region of the *Chlamydomonas* cyt b_6f structure (2) are shown in Fig. 2. The first three N-terminal residues (Ala^1 to Ala^3) and the flexible hinge (Ser^{43} to Gly^{50}) of the Rieske ISP are not resolved in the structure (2), very likely because of their flexibility, and are not shown in Fig. 2. The eight-residue-long flexible hinge of the *Chlamydomonas* chloroplast Rieske protein contains two serine residues followed by a stretch of six glycines (Fig. 1). This domain is required for the ISP conformational movement. We modified the length of this domain by the addition of 1, 3, or 5 glycines (mutations +1G, +3G, and +5G) or deletion of 1 or 3 glycines (mutations Δ1G and Δ3G). In the PetC-Δ4 mutant we deleted 4 residues, Ala-Ser-Ser-Glu (ASSE), from the already short N-terminal domain to test the role of this domain in signaling.

A characteristic feature of the cyt b_6f complex is the absence of a charged residue (lysine or arginine) at the lumenal end the Rieske ISP transmembrane helix. Such charged residues at the ends of transmembrane helices serve to anchor these helices to the membrane and are found in the cyt bc_1 ISP counterpart (*arrow* on Fig. 1). To test whether the absence of this charged residue in the cyt b_6f ISP represents an important feature for function of the cyt b_6f complex, we generated a mutant strain (A32K) where a polar residue has been introduced into the lumenal end of the ISP helix (Figs. 1 and 2). In the cyt b_6f structures (2, 3), the N-terminal domain of the Rieske protein lies close to the C-terminal domain of cyt *f*. In the *Chlamydomonas* structure, an endogenous sulfolipid (sulfoquinovosyldiacylglycerol (SQDG)) interacts via hydrogen bonds with Rieske protein Arg^{13} and Asn^{17} and cyt *f* Lys^{272}. Residues Arg^{13} and Asn^{17} are conserved in cyt b_6f Rieske proteins (Fig. 1). To test the role of Asn^{17} in proton translocation and/or possible assembly-mediated control of cyt *f* synthesis, we decreased the polarity of this residue by constructing the substitution N17V (see *N17V* in Figs. 1 and 2).

Rieske ISP Hinge Mutants; Assembly of the cyt b_6f Complex and Electron Transfer Properties—To further investigate the relationship between Rieske ISP flexibility and function in the cyt b_6f complex, we extended the mutational approach to include insertions of up to 5 residues and deletions of up to 3 residues. Previous ISP hinge mutations (in cyanobacteria) were limited to insertion of 4 residues and deletions of 1 or 2 residues. The two-residue deletion slowed electron transfer by a factor of four (16).

The results of immunodetection analysis indicated that the cyt b_6f subunits accumulated to wild type (WT) levels in all of the flexible hinge mutants even though their Rieske proteins were of different size (Fig. 3). Spectroscopic analysis of the modified cyt b_6f complex *in vivo* (Table I) confirmed the high tolerance of the ISP hinge for modifications in length. A dramatic consequence on electron transfer was observed only in the Δ3G mutant (three residues deletion of the hinge). The effect of this mutation (Fig. 4; note the differences in times scales on the *abscissa* between WT in A/B/C and Δ3G-1 in D/E/F) was to reduce in a concerted manner the rate of electron injection into both the high potential pathway, as evidenced by the kinetics of cyt *f* reduction (Fig. 4, *panels B* and *E*) and the low potential chain. The latter pathway was monitored by measuring the slow phase of the electrochromic signal (the "b phase," *panels A* and *D*), which results from electron transfer between the *b* hemes. In addition, redox changes of the *b* hemes were measured directly (*panels C* and *F*). Cyt b_6 redox kinetics are rather complex, resulting from cyt b_L reduction by PQH_2 from the Q_o-site, cyt b_L oxidation by cyt b_H, and then cyt b_H oxidation by plastoquinone at the Q_i site. To directly monitor cyt b_L reduction, which is linked to plastoquinol oxidation, kinetics were measured in the presence of the inhibitor 2-*N*-4-hydroxyquinoline-*N*-oxide. This compound selectively slows down cyt b_H oxidation at the Q_i site (37) and allows a correct deconvolution of the reduction signal (triangles in *panels C* and *F*).

It is known that a proton gradient exists across the thylakoid membranes of dark adapted *Chlamydomonas* cells. This gradient arises from ATP hydrolysis by the CF0-F1 ATP synthase-ATPase complex (34). The gradient slows down the kinetics of plastoquinol oxidation at the Q_o site. In the Δ3G mutant, the consequences of the electrochemical proton gradient on cyt b_6f catalysis were larger than in the wild type; the rates of PQH_2 oxidation were 12 and 50 times slower than in wild type cells in the presence and absence of the protonophore FCCP, respectively. This phenotype resembles that of two other cyt b_6f mutants of *Chlamydomonas*; FUD2, in which the Q_o site of the cyt b_6f is modified because of a 36-base pair duplication in the cd loop of cyt b_6 (34), and *ycf*7, where the PetL subunit is disrupted (38). Both of these mutants show loosened binding of the Rieske protein to the cyt b_6f complex. We, therefore, tested whether a similar perturbation of ISP binding could be observed in the Δ3G mutant. To this aim, cyt b_6f complexes were purified from exponentially growing cells of the Δ3G mutant using the Hecameg solubilization procedure described in Pierre *et al.* (29). The distributions of cyt *f* and Rieske proteins upon gradient centrifugation peaked in the same fractions and were similar for the Δ3G and wild type strains (Fig. 5). These results indicate that Rieske protein binding to the b_6f complex was not

TABLE I
Functional properties of the Rieske ISP mutants
ND, not determined.

Strain phototrophy		$t_{½}$-ms phase b[a]		$t_{½}$-ms re-reduction cyt *f*	
		+FCCP	−FCCP	+FCCP	−FCCP
+5G	+	4.2	10	4	9
+3G	+	4.1	ND	ND	ND
+1G	+	3.6	ND	ND	ND
WT	+	2.4	7	2.7	6
Δ1G	+	2.0	ND	ND	ND
Δ3G	+/−	29	—[b]	33	300
ΔpetC[c]	−	—[b]	—[b]	10,000	ND
Δ4 (N terminus)	+	2.0	ND	ND	ND
N17V	+	2.0	ND	ND	ND
A32K	+	2.0	ND	ND	ND

[a] Phase b of the electrochromic shift of carotenoids was measured at 515 nm with non-saturating flashes in the presence or absence of 1 μM FCCP.
[b] Kinetics are too slow to be deconvoluted from the field decay.
[c] Deletion that eliminates the Rieske protein (26).

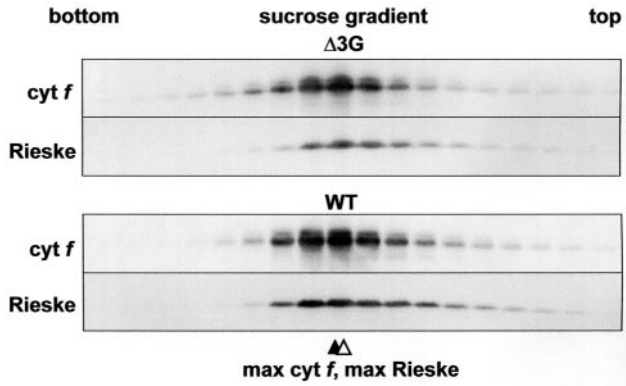

FIG. 5. **Binding of the Rieske protein to the b_6f complex is not loosened in the Δ3G mutant.** Thylakoid membranes were solubilized with HG. The supernatant was centrifuged on a 10–30% sucrose gradient. Fractions of the gradient were collected, analyzed by SDS-PAGE (12–18% acrylamide, 8 M urea), and immunodetected.

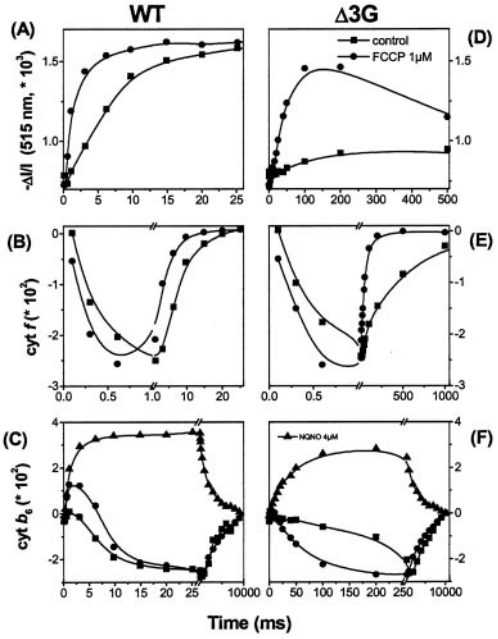

FIG. 4. **Kinetics of the electrochromic signal (*A* and *D*), cyt *f* (*B* and *E*), and cyt b_6 (*C* and *F*) redox changes in the WT (*A*, *B*, and *C*) and Δ3G mutant (*D*, *E*, and *F*).** Algae were collected during exponential growth phase and resuspended in Hepes 20 mM, pH 7.2, buffer with the addition of 20% (w/v) Ficoll to prevent sedimentation. Cells were illuminated with non-saturating actinic flashes of red light at a frequency of 0.15 Hz. 3-(3′,4′-dichloroprenyl)-1–1-dimethylurea and hydroxylamine were added at concentrations of 10 μM and 1 mM, respectively, to block PSII activity. Where indicated, FCCP was added at the concentration of 1 μM to facilitate pH equilibration between the chloroplast compartments. 2-*N*-4-hydroxyquinoline-*N*-oxide (*NQNO*) was added at the concentration of 4 μM to slow plastoquinone reduction at the Q_i site. The fast and slow phases of the electrochromic signal in *panels A* and *D* represent charge separation within PSI and the cyt b_6f complex, respectively. In *panels B*, *C*, *E*, and *F*, upward and downward absorption changes correspond to reduction and oxidation of the cyt b_6f redox cofactors, respectively. $-\Delta I/I$ is the difference between the light transmitted through the measuring and reference cuvettes divided by the light transmitted through the reference cuvette.

loosened in the Δ3G mutant. Therefore, the large sensitivity of the electron transfer rate to an electrochemical proton gradient appears to have a different physical basis in the Δ3G mutant than in the FUD2/*ycf7*mutants.

Rieske ISP Hinge Mutants; Structural Changes and LHC Kinase Activation—The strong kinetic effect measured in the Δ3G mutant, which has a catalytic rate 50 times slower than the wild type in the presence of the electrochemical proton gradient, offered an opportunity to test the possible consequences of a decreased hinge flexibility on the efficiency of LHC kinase activation. To perform such a study, fluorescence emission was measured at room temperature in intact algae upon adaptation to anaerobiosis. 3-(3′,4′-Dichloroprenyl)-1–1-dimethylurea was added to prevent PSII photochemistry. This allowed an estimation of the fraction of antenna connected to PSII directly from fluorescence emission changes. Algae in state II (see "Materials and Methods") were submitted to illumination to promote transition to state I. Subsequently, their recovery to state II was followed in the dark. This procedure was adopted (35) to distinguish between the intrinsic state I-state II transition rate and that of plastoquinone reduction, which often limits the overall process of state II transition upon adaptation of the algae to anaerobiosis.

No significant differences were observed in the ability to perform a state I-state II transition of the wild type and the Δ3G mutant (we calculated values of 60 ± 22 s for this transition in the wild type (mean of 6 different experiments) and 72 ± 14 s (4 experiments) for the Δ3G mutant) nor of any of the other ISP hinge mutants (not shown). No state II transition was observed in the ΔpetC strain (lacking the chloroplast ISP), likely because of its blockage in plastoquinol binding. Consistent with the fluorescence measurements, a wild type pattern of antenna protein phosphorylation was observed in the Δ3G and +5G mutants (Fig. 6). In contrast and regardless of the state condition, the ΔpetC mutant displayed a low and constant level of phosphorylation of LHC proteins CP26, CP29, and p11 and an absence of phosphorylation of LHC proteins p13, p17, and cyt b_6f subunit PetO (39)). This condition is typical of state I.

Rieske Protein Mutants in the Stromal and Transmembrane Domains—Neither the Δ4 mutant (deletion of 4 residues from the N-terminal domain) nor the A32K mutant (insertion of a polar residue at the lumenal end of the ISP transmembrane helix) displayed any remarkable phenotype with respect to accumulation of the cyt b_6f complex (Fig. 7), electron transport (Table I), or state transitions (not shown). On the other hand a significant decrease in the accumulation of cyt b_6f subunits was observed in both the ΔpetC and the N17V mutants (Fig. 7*A*). The rates of synthesis and membrane insertion during a 5-min pulse labeling of cyt b_6 and subunit IV were very similar in the N17V and ΔPetC mutants and the wild type (Fig. 7*C*). The rate of synthesis and membrane insertion of the Rieske ISP during an 8-min pulse-labeling showed no differences between the wild type and the N17V mutant but showed an absence of label incorporation into Rieske protein (as expected) in the ΔpetC

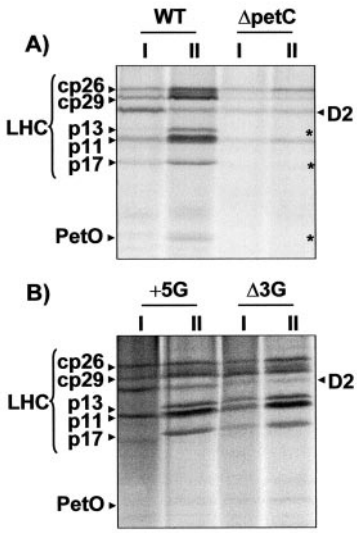

FIG. 6. **Autoradiogram of ^{33}P-radiolabeled polypeptides.** Protein are shown in the 15–35-kDa range. *A*, thylakoid membrane proteins of WT strain and Rieske protein deletion mutant (Δ*petC*). *B*, thylakoid membrane proteins of Rieske protein hinge insertion (+5G) and deletion (Δ3G) mutants. Cells were placed in state I (*I*) or state II (*II*) conditions. *Stars* indicate the absence of phosphorylation.

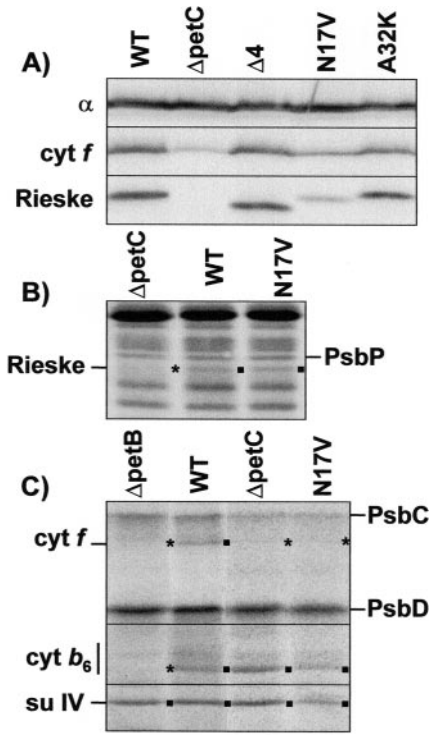

FIG. 7. **Accumulation and synthesis rates of cyt b_6f subunits in Rieske ISP N-terminal and transmembrane domain mutants.** *A*, immunodetection of cyt *f* and Rieske protein in mutant cells from exponential growing phase; accumulation of the α subunit of CF_1 provided a loading control. *B*, cytoplasmic pulse-labeled, translation products. *C*, chloroplast pulse-labeled translation products. Whole cells from Rieske ISP deletion (Δ*petC*) and N17V substitution (*N17V*) mutants, WT, and cyt b_6-deficient (Δ*petB*) mutant strains were pulse-labeled with [^{14}C]acetate for either 8 min in the presence of an inhibitor of chloroplast translation or for 5 min in the presence of an inhibitor of cytoplasmic translation. Thylakoid membrane proteins were separated by SDS-PAGE (12–18% acrylamide, 8 M urea). *Stars* indicate the absence or large decrease of rate of synthesis of a translation product. *Black squares* indicate translation products of the major b_6f subunits. Psb defines various PSII subunits.

mutant (Fig. 7*B*). Still, the lower accumulation of the Rieske protein in the N17V mutant was not due to a higher proteolytic susceptibility of the assembled Rieske protein since it remained as stable in N17V as in wild type over 6 h, in an immunodetection experiment where the amount of Rieske protein at various time points after the addition of an inhibitor of cytoplasmic translation was probed *in vivo* with specific antibodies (not shown). These observations argue for a rapid degradation of a fraction of neosynthesized Rieske before its assembly in cyt b_6f complexes in the N17V mutant.

In ΔpetB (lacking cyt b_6), ΔpetC, and N17V mutants, there was a large decrease in the rate of cyt *f* synthesis, down to the limit of detection (see the *stars* in Fig. 7*C*). The rate of cyt *f* synthesis decreased by a factor of 3 in the ΔpetC and N17V mutants as compared with a factor of 10 in the ΔpetB mutant. This has been attributed previously to an assembly-mediated control of cyt *f* synthesis (40). These data reveal a new role for the Rieske ISP transmembrane helical domain; namely, as an additional partner involved in assembly-mediated control of cyt *f* synthesis.

DISCUSSION

The Rieske Fe_2S_2 protein is actively involved in forming the quinol binding site in both bc_1 and b_6f cyt complexes. Moreover, it plays a direct role in catalysis by means of the large movement of the Rieske cluster domain, which is linked to the membrane via a flexible hinge. The same movement has been implicated in the transduction of the activating signal from the Q_o site to the LHCII kinase during state transitions. In the current work we have addressed in detail the involvement of the Rieske protein in these two major processes by generating site-specific mutations in the flexible hinge, the transmembrane helix, and the N-terminal, stromal-exposed domain. We have also investigated the role of the Rieske ISP in regulation of the assembly of the cyt b_6f complex.

The Flexible Hinge of the b_6f Rieske Protein Is More Tolerant to Insertions than Deletions—The b_6f Rieske ISP hinge of Chlamydomonas contains a string of six glycines. We have varied the number of consecutive glycines in the hinge from 11 (+5G) to 3 (Δ3G). All the generated mutants correctly assembled the cyt b_6f complex, and only one of them (Δ3G) showed a reduction in the catalytic efficiency of the complex. This supports and extends previous findings, indicating a large tolerance of the flexible hinge of the b_6f Rieske protein to structural changes (16, 26). At the same time we show here that it is indeed possible to severely lower the efficiency of electron flow in the cyt b_6f complex by a modification of the Rieske hinge. The Δ3G mutation slowed catalysis by a factor of ~10-fold. Consistent with the severe consequences of extended deletions, we could not select by restoration of phototrophy a Δ5G mutation (data not shown). Therefore, despite the greater flexibility of the cyt b_6f Rieske protein hinge, modifications that prevent ISP conformational changes have clearly deleterious consequences on catalytic efficiency in both b_6f and bc_1 cyt complexes. These data are consistent with a requirement for Rieske ISP conformational mobility in cyt b_6f complexes.

The b_6f ISP subunit can tolerate large modifications of its flexible hinge, particularly increases in length, without compromising catalytic efficiency (Refs. 16 and 26 and this work). This is not the case in the bc_1 ISP counterpart (for review, see Ref. 11). The differing degrees of flexibility of the Rieske ISP hinge observed in bc_1 and b_6f complexes are consistent with the three-dimensional structures of these complexes. In the former the hinge is clearly defined. It is extended when the Fe_2S_2 cluster resides in the proximal (Q_o) position and in a helical conformation when the cluster occupies the distal (cyt c_1) position (7–9, 41). No structures are available for different conformations of the cyt b_6f Rieske ISP subunit. Nevertheless, the

hinge region is clearly less well defined. The hinge assumes an intermediate conformation between the proximal and the distal positions in one of the available structures (3) and is not resolved in the other (2) because of a very large degree of freedom.

The Rieske Protein Is Required for Kinase Activation, but Its Rapid Movement Is Not Limiting—The Rieske ISP deletion mutant ΔpetC is locked in a state I condition. This likely arises from a nonfunctional Q_o site that, therefore, does not allow activation of the LHCII kinase. This phenotype is in agreement with previous findings, showing that binding of plastoquinol to the Q_o site is essential for signal transduction during state transitions (19–21).

In contrast, the Δ3G mutant, where plastoquinol oxidation was very slow because of the truncated ISP hinge, did not show any significant alteration in the kinetics of state I-state II transitions. In principle, this result might suggest that the movement of the Rieske ISP does not play any role in state transitions. However, even in the Δ3G mutant, the rate of electron transfer (and, therefore, the rate of Rieske ISP conformational changes) is at least 2 orders of magnitude faster than the rate of the state I-state II transition itself. This rate may be governed primarily by the kinetic properties of the kinase itself (35), although LHCII lateral diffusion in thylakoid membranes has also been implicated (see *e.g.* Ref. 42). Therefore, we conclude that as long as conformational changes related to plastoquinol binding to the Q_o site remain faster than the limiting step of state transitions, the latter process can take place efficiently even in the presence of a severely crippled Q_o site. This is consistent with the phenotype of the *Chlamydomonas* FUD2 mutant, where electron flow is slowed ~8-fold by a reduced binding affinity of plastoquinol for the Q_o site, but state transitions remain unaffected (34).

A central, unresolved issue in chloroplast state transitions and perhaps redox signaling more generally is the pathway employed to transduce the activating signal from the lumen, where plastoquinol binds to the Q_o site, to the stroma, where the catalytic domain of the kinase resides. Several hypotheses have been formulated. (i) An LHCII kinase might be activated through a direct interaction between its transmembrane helix and the Q_o site (22). (ii) A transmembrane conformational change within the b_6f complex might carry the signal (23), as supported by subunit IV-PetL fusion experiments (43), (iii) perhaps via chlorophyll or β-carotene molecules, as suggested in Stroebel *et al*. (2), or (iv) alternatively, via conformational changes within the Rieske ISP itself. In this study, we have rendered the latter hypothesis less likely by modifying several domains of the Rieske ISP without altering state transitions.

Role of the Rieske ISP and a Sulfolipid in Assembly-mediated Control of cyt f Synthesis—We have previously shown that the Rieske protein deletion mutant ΔpetC accumulates a lower amount of cyt b_6f complex than the wild type (26). The steady state accumulation of cyt b_6f complex in the ΔpetC mutant is increased when the ClpP protease expression is attenuated (44). Therefore, part of the diminished level of cyt b_6f accumulation can be attributed to proteolytic degradation. In addition, cyt *f* accumulation is regulated by an "assembly-mediated control" process that results in markedly decreased cyt *f* synthesis in the absence of the large, chloroplast-encoded cyt b_6 and subunit IV components of the cyt b_6f complex (40). This process, termed CES (control by epistasy of synthesis), occurs by the autoregulation of cyt *f* translation via the 5′-untranslated region of *petA* (cyt *f*) mRNA (45) and the cyt *f* protein C-terminal domain (46). The proximity of the N-terminal Rieske ISP transmembrane helix and the cyt *f* C-terminal transmembrane helix in the cyt b_6f structures (2, 3) suggested that the Rieske protein might also play a more direct role in this process. Consistent with this idea, we observed a 3-fold decrease of cyt *f* synthesis in the Rieske-protein− mutant, ΔpetC, similar to that reported previously (47). This decrease is less pronounced than the 10-fold decrease in cyt *f* synthesis observed in the absence of the cyt b_6 and subunit IV proteins (40) but clearly points to a role for the Rieske protein in assembly-mediated control of cyt *f* synthesis.

The rate of synthesis of the Rieske protein is not affected in N17V mutant. The lower accumulation of the N17V Rieske protein should be attributed to a rapid degradation of unassembled ISP rather than to a higher susceptibility to proteases of the assembled N17V variant of the Rieske ISP that proved as stable as in the wild type over 6 h. The lower rate of cyt *f* synthesis in the N17V mutant suggests that, although most of the neosynthesized Rieske ISP assembles in cyt b_6f complexes, there is a modified conformation of its transmembrane helix due to the N17V substitution that allows assembled cyt *f* to exert some negative control of its own synthesis. Indeed, the *Chlamydomonas* b_6f structure reveals the presence of an endogenous sulfolipid SQDG that interacts with Rieske protein residues Arg^{13} and Asn^{17} and cyt *f* Lys^{272} (see Fig. 2). Lys^{272} has been established as a key residue in the control of cyt *f* synthesis (46). The R13K mutation (48) is semiconservative; it substitutes a basic residue by another basic residue that should still allow the hydrogen bond formation with SQDG, and it did not affect the rate of cyt *f* synthesis (not shown). In contrast, N17V mutation substitutes a polar residue by a non-polar residue, which prevents the hydrogen bond formation with SQDG; in N17V mutant, the rate of cyt *f* synthesis is clearly decreased. This suggests that the region delimited by the endogenous sulfolipid, the Rieske protein, and the cyt *f* helix plays a specific role in the assembly-mediated control of cyt *f* synthesis. It is tempting to speculate that removal of the Rieske protein or modification of its binding to the sulfolipid would increase the accessibility of the cyt *f* target domain to the trans-acting factors that regulate translation of cyt *f* (46, 49).

Sulfolipids are known to play major roles in photosynthetic membranes. The sulfolipid SQDG is crucial for photosynthesis in *Synechocystis* sp. PCC 6803 (50). The growth of a sulfolipid-deficient *Arabidopsis* mutant is impaired after phosphate starvation (51). A double mutant of *Arabidopsis* lacking SQDG and phosphatidylglycerol is impaired in PSII activity and photosynthetic growth (52). Several *Chlamydomonas* mutants lacking SQDG have altered PSII activity or structural integrity (53–55) including the D1 protein as a major target (56). Therefore, SQDG seems to be involved in the turnover of both D1 and cyt *f*. The synthesis of both subunits is modulated by the presence of their assembly partners. This raises the interesting question of whether a similar mechanism underlies the role of SQDG in the assembly of both subunits and, as a consequence, in the operation of the CES process.

Acknowledgements—We gratefully acknowledge C. Facciotti as a recipient of a European Economic Community Erasmus scholarship for participation in Rieske ISP mutagenesis, F. Zito for *in vivo* phosphorylation labeling expertise, D. Picot and D. Stroebel for stimulating discussions and privileged communication of the *Chlamydomonas* cyt b_6f structure, and Y. Choquet for critical reading of the manuscript.

REFERENCES

1. Berry, E. A., Guergova-Kuras, M., Huang, L.-S., and Crofts, A. R. (2000) *Annu. Rev. Biochem.* **69,** 1005–1075
2. Stroebel, D., Choquet, Y., Popot, J.-L., and Picot, D. (2003) *Nature* **426,** 413–418
3. Kurisu, G., Zhang, H., Smith, J. L., and Cramer, W.A. (2003) *Science* **302,** 1009–1014
4. de Vitry, C., Desbois, A., Redeker, V., Zito, F., and Wollman, F.-A. (2004) *Biochemistry* **43,** 3956–3968
5. Mitchell, P. (1975) *FEBS Lett.* **59,** 137–139
6. Crofts, A. R., Meinhardt, S. W., Jones, K. R., and Snozzi, M. (1983) *Biochim. Biophys. Acta* **723,** 202–218
7. Xia, D., Yu, C.-A., Kim, H., Xia, J.-Z., Kachurin, A. M., Zhang, L., Yu, L., and

Deisenhofer, J. (1997) *Science* **277,** 60–66
8. Zhang, Z., Huang, L., Shulmeister, V. M., Chi, Y.-I., Kim, K. K., Hung, L.-W., Crofts, A. R., Berry, E. A., and Kim, S.-H. (1998) *Nature* **392,** 677–684
9. Iwata, S., Lee, J. W., Okada, K., Lee, J. K., Iwata, M., Rasmussen, B., Link, T., Ramaswamy, S., and Jap, B. K. (1998) *Science* **281,** 64–71
10. Brugna, M., Rodgers, S., Schricker, A., Montoya, G., Katzmeier, M., Nitschke, W., and Sinning, I. (2000) *Proc. Natl. Acad. Sci. U. S. A.* **97,** 2069–2074
11. Darrouzet, E., Moser, C.C., Dutton, P.L., and Daldal, F. (2001) *Trends Biochem. Sci.* **26,** 445–451
12. Breyton, C. (2000) *Biochim. Biophys. Acta* **1459,** 467–474
13. Heimann, S., Ponamarev, M. V., and Cramer, W. A. (2000) *Biochemistry* **39,** 2692–2699
14. Soriano, G. M. Guo, L. W., de Vitry, C., Kallas, T., and Cramer, W. A. (2002) *J. Biol. Chem.* **277,** 1865–1871
15. Schoepp, B., Brugna, M., Riedel, A., Nitschke, W., and Kramer, D. M. (1999) *FEBS Lett.* **450,** 245–250
16. Yan, J., and Cramer, W. A. (2003) *J. Biol. Chem.* **278,** 20925–20933
17. Wollman, F. A. (2001) *EMBO J.* **20,** 3623–3630
18. Allen, J. F. (1992) *Biochim. Biophys. Acta* **1098,** 275–335
19. Vener, A. V., van Kan, P. J., Gal, A., Andersson, B., and Ohad, I. (1995) *J. Biol. Chem.* **270,** 25225–25232
20. Vener, A. V., van Kan, P. J., Rich, P., Ohad, I., and Andersson, B. (1997) *Proc. Natl. Sci. Acad. U. S. A.* **94,** 1585–1590
21. Zito, F., Finazzi, G., Delosme, R., Nitschke, W., Picot, D., and Wollman, F.-A. (1999) *EMBO J.* **18,** 2961–2969
22. Vener, A. V., Ohad, I., and Andersson, B. (1998) *Curr. Opin. Plant Biol.* **1,** 217–223
23. Finazzi, G., Zito, F., Barbagallo, P. R., and Wollman, F.-A. (2001) *J. Biol. Chem.* **276,** 9770–9774
24. Fleischmann, M. M., Ravanel, S., Delosme, R., Olive., J., Zito, F, Wollman, F. A., and Rochaix J.-D. (1999) *J. Biol. Chem.* **274,** 30987–30994
25. Depège, N., Bellafiore, S., and Rochaix, J.-D. (2003) *Science* **299,** 1572–1575
26. de Vitry, C., Finazzi, G. Baymann, F., and Kallas, T. (1999) *Plant Cell* **11,** 2031–2044
27. Kropat, J., von Gromoff, E. D., Müller, F. W., and Beck, C. F. (1995) *Mol. Gen. Genet.* **248,** 727–734
28. Breyton, C., de Vitry, C., and Popot, J.-L. (1994) *J. Biol. Chem.* **269,** 7597–7602
29. Pierre, Y., Breyton, C., Kramer, D., and Popot, J.-L. (1995) *J. Biol. Chem.* **270,** 29342–29349
30. Lemaire, C., Girard-Bascou, J., Wollman, F.-A., and Bennoun, P. (1986) *Biochim. Biophys. Acta* **851,** 229–238
31. Wollman, F.-A., and Delepelaire, P. (1984) *J. Cell Biol.* **98,** 1–7
32. Bulté, L., Gans, P., Rebéillé, F., and Wollman, F.-A. (1990) *Biochim. Biophys. Acta* **1020,** 72–80
33. Joliot, P., and Joliot, A. (1994) *Proc. Natl. Acad. Sci. U. S. A.* **91,** 1034–1038
34. Finazzi, G., Büschlen, S., de Vitry, C., Rappaport, F., Joliot, P., and Wollman, F.-A. (1997) *Biochemistry* **36,** 2867–2874
35. Delepelaire, P., and Wollman, F.-A. (1985) *Biochim. Biophys. Acta* **809,** 277–283
36. de Vitry, C. (1994) *J. Biol. Chem.* **269,** 7603–7609
37. Selak, M. A., and Whitmarsh, J. (1982) *FEBS Lett.* **150,** 286–292
38. Takahashi, Y., Rahire, M., Breyton, C., Popot, J.-L., Joliot, P., and Rochaix, J.-D. (1996) *EMBO J.* **15,** 3498–3506
39. Hamel, P., Olive, J., Pierre, Y., Wollman, F.-A., and de Vitry, C. (2000) *J. Biol. Chem.* **275,** 17072–17079
40. Kuras, R., and Wollman, F.-A. (1994) *EMBO J.* **13,** 1019–1027
41. Hunte, C., Koepke, J., Lange, C., Rossmanith, T., and Michel, H. (2000) *Structure* **8,** 669–684
42. Drepper, F., Carlberg, I., Andersson, B., and Haehnel, W. (1993) *Biochemistry* **32,** 11915–11922
43. Zito, F., Vinh, J., Popot, J.-L., and Finazzi, G. (2002) *J. Biol. Chem.* **277,** 12446–12455
44. Majeran, W., Wollman, F.-A., and Vallon, O. (2000) *Plant Cell* **12,** 137–149
45. Choquet, Y., Stern, D. B., Wostrikoff, K., Kuras, R., Girard-Bascou, J., and Wollman, F.-A. (1998) *Proc. Natl. Acad. Sci. U. S. A.* **95,** 4380–4385
46. Choquet, Y., Zito, F., Wostrikoff, K., and Wollman, F.-A. (2003) *Plant Cell* **15,** 1445–1454
47. Majeran, W. (2002) *La Protéolyse dans le Chloroplaste de Chlamydomonas reinhardtii: Rôle et Organization Structurale de la Protéase ClpP.* Ph.D thesis, Institut National Agronomique Paris-Grignon
48. Finazzi, G., Chasen, C., Wollman, F.-A., and de Vitry, C. (2003) *EMBO J.* **22,** 807–815
49. Wostrikoff, K., Choquet, Y., Wollman, F.-A., and Girard-bascou, J. (2001) *Genetics* **159,** 119–132
50. Aoki, M., Sato, N., Meguro, A., and Tsuzuki, M. (2004) *Eur. J. Biochem.* **271,** 685–693
51. Yu, B., Xu, C., and Benning, C. (2002) *Proc. Natl. Sci. Acad. U. S. A.* **99,** 5732–5737
52. Yu, B., and Benning, C. (2003) *Plant J.* **36,** 762–770
53. Sato, N., Sonoike, K., Tsuzuki, M., and Kamaguchi, A. (1995) *Eur. J. Biochem.* **234,** 16–23
54. Riekhof, W. R., Ruckle, M. E., Lydic, T. A., Sears, B. B., and Benning, C. (2003) *Plant Physiol.* **133,** 864–874
55. Sato, N., Aoki, M., Maru, Y., Sonoike, K., Minoda, A., and Tsuzuki, M. (2003) *Planta* **217,** 245–251
56. Minoda, A., Sonoike, K., Okada, K., Sato, N., and Tsuzuki, M. (2003) *FEBS Lett.* **553,** 109–112